

Elastic-Plastic Analysis of Space Trusses with Large Displacements

¹*Vera V. Galishnikova, ²Evgeny V. Lebed

¹ Peoples' Friendship University of Russia (RUDN University), Moscow, Russia

² Moscow State University of Civil Engineering, Moscow, Russia

* Corresponding Author: galishni@gmail.com

<https://doi.org/10.26782/jmcms.2019.03.00027>

Abstract

Analysis of spatial bar structures is a labor-intensive and complex task, and it must be carried out taking into account all possible limiting states in various operating conditions of structures. The aim of this paper is to give an insight into elastic-plastic analysis that enables determining the ultimate load of space trusses with large displacements. A direct method is treated in this investigation to gain insight into the computational effort required for the method. The algorithms for the direct methods are obtained by modifying the algorithms for incremental geometrically nonlinear analysis developed by one of the authors to account for yielding and plastic deformation in the bars of the truss. A Java software application has been developed based on the algorithms and the analysis of the space arch truss has been performed. The example demonstrates that direct limit analysis of space trusses with large displacements can be implemented successfully on the Java platform. The computer application is suitable as a test platform for a broad spectrum of investigations into elastic-plastic truss behavior.

Keywords : Steel Space Trusses, Geometrical Nonlinearity, Elastic-Plastic Analysis, Limit State, Direct Method

I. Introduction

The research which is described in this paper deals with the geometrically nonlinear stress and stability analysis of elastic space trusses undergoing large displacements. The aim of this paper is to give an insight into elastic-plastic analysis whose aim it is to determine the ultimate load of space trusses with large displacements. While a Java application has been developed to analyze the examples in this appendix, a complete investigation of elastic-plastic analysis lies outside the scope of the paper and has not been conducted. Two basic methods have been developed in the literature for elastic-plastic analysis: the optimization method and the direct method. In the solution by optimization, a sequence of statically admissible

states of the structure is studied to determine a maximum load factor. Alternately a sequence of kinematically admissible states of the structure is studied to determine a minimum load factor. In the direct method, both the kinematic and the static conditions are satisfied simultaneously so that optimization is not required.

The direct method requires the analysis of a sequence of configurations of the structure because plasticity changes the stiffness of a structure. After each yielding of a bar in a truss, or if a plastic bar becomes elastic due to unloading, the stiffness matrix must be reassembled and decomposed. The required computational capacity was not available when the early research was performed. Preference was therefore given to the optimization method for which a set of theorems was developed.

All theorems on which the optimization method is based depend on the linear superposition of load cases to form load combinations (Heidari, Galishnikova, 2014). If the behavior of a structure is geometrically nonlinear load cases cannot be superimposed. For such structures the theorems of the optimization method are not valid and the optimization approach cannot be used for the limit analysis. Given the present capacity of computers, it is not obvious even for problems with small displacements that the indirect optimization method is today still preferable to the direct method.

A direct method will be treated in this paper to gain insight into the computational effort required for the method. The algorithms are developed by modifying the algorithms by one of the authors (Galishnikova, 2015) to account for yielding and plastic deformation.

Elastic-Plastic Behavior of a Steel Bar

Each bar of the truss is treated as a straight finite element of constant cross-section subject only to an axial force. The bar is pin-connected to a node at each end. Euler buckling of the pinned elastic bar is neglected. If the bar is plastic, it is assumed that the bar can carry the axial yield force.

It is assumed that the each bar of the truss is either in a perfectly elastic state or in a perfectly plastic state throughout each load step. The step size is determined in the solution algorithm such that this assumption is justified. The contribution of an elastic bar to the secant stiffness matrix of the truss is determined with the formulas for geometrically nonlinear space truss analysis [xxx]. If the bar is plastic its contribution to the secant stiffness matrix of the truss is null.

Figure 1 shows possible changes of state of a bar as a function of the axial strain increment in a load step. At points A, D and G the bar is elastic for positive and negative strain increments. At points B and C the bar is plastic for positive strain increments and elastic for negative strain increments. At points E and F the bar is elastic for positive strain increments and plastic for negative strain increments.

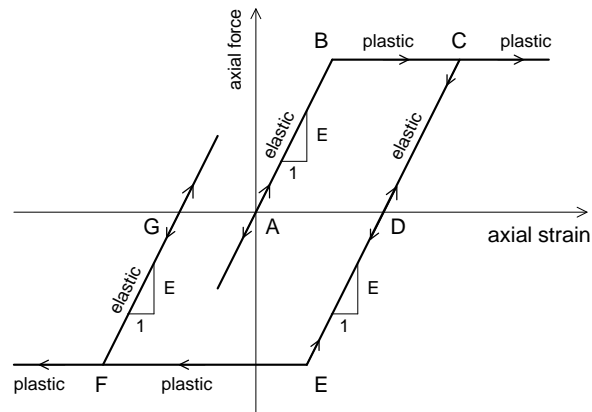


Fig. 1. Variation of axial bar force with axial strain

Let $\varepsilon_t, \varepsilon_e$ and ε_p be the total, elastic and plastic strain in the bar respectively. Let superscript (s) denote the value of a variable at the start and superscript (t) its value at the end of the load step. Let v_k be the components of the coordinates of the displacement in the reference coordinate system and $v_{k,1}$ the derivative with respect to the axial coordinate y_1 . The total axial strain in the bar is given by (Galishnikova, 2009):

$$\varepsilon_t = v_{1,1} + \frac{1}{2}(v_{1,1}^2 + v_{2,1}^2 + v_{3,1}^2) \quad (1)$$

If the bar is elastic in the load step, its strain in the trial state is given by:

$$\varepsilon_e^{(t)} = \varepsilon_t^{(t)} - \varepsilon_p^{(s)}; \quad \varepsilon_p^{(t)} = \varepsilon_p^{(s)}. \quad (2)$$

Let m be the conversion factor between 2.Piola-Kirchhoff and engineering stress coordinates. The stress σ and the axial bar force f in the trial state are given by (Galishnikova, 2009):

$$\begin{aligned} m &= \sqrt{(1 + v_{1,1})^2 + v_{2,1}^2 + v_{3,1}^2} \\ \sigma^{(t)} &= m^{(t)} E \varepsilon_e^{(t)} \\ f^{(t)} &= A \sigma^{(t)} \end{aligned} \quad (3)$$

If the bar is plastic in the load step, its strain in the trial state is given by:

$$\begin{aligned} \varepsilon_e^{(t)} &= \varepsilon_e^{(s)} \\ \varepsilon_p^{(t)} &= \varepsilon_p^{(s)} + V \varepsilon_p \quad \text{with } V \varepsilon_p = \varepsilon_t^{(t)} - \varepsilon_t^{(s)} \end{aligned} \quad (4)$$

The stress σ and the axial force f in a plastic bar are given by:

$$\begin{aligned} \sigma^{(t)} &= \sigma^{(s)} \\ f^{(t)} &= f^{(s)} \end{aligned} \quad (5)$$

Direct Method of Limit Analysis

In the direct method of limit analysis a load pattern is prescribed and multiplied by a load factor λ to obtain the applied load. The maximum value of the load factor is determined for which the structure is stable. Since the displacements are assumed to be large, it is not known at the outset whether instability will be due to buckling or due to a plastic mechanism.

The workflow for the limit load analysis of a truss is shown in figure 2. The diagram accounts for both geometric and physical nonlinearity. The algorithm consists of two nested loops. The outer loop traverses the load steps until a specified load factor has been reached or a limit state of the truss is detected. In the inner loop the secant stiffness matrix for a load step is computed iteratively accounting for the displacement increments and the changes of state of the bars.

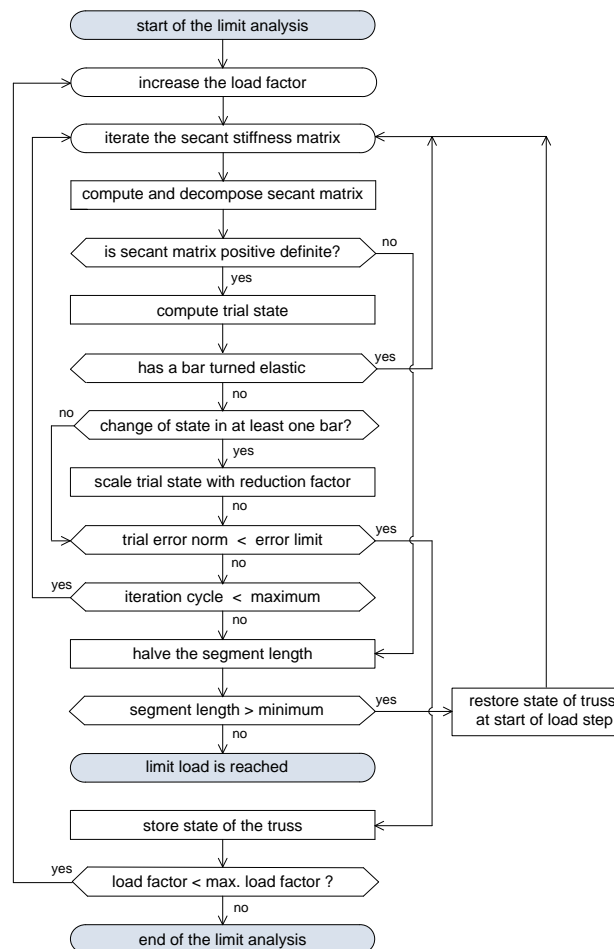


Fig. 2. Work flow of the limit load analysis of a truss

The true state of the bars in a load step is determined iteratively. At the start of load step 0 all bars are elastic and free of stress. In the first cycle of iteration in all other load steps, it is assumed that a bar is plastic if was plastic at the end of the previous load step. Otherwise the bar is assumed to be elastic. These assumptions may not be correct and will be corrected if necessary at the end of the load step.

In the first cycle of iteration the tangent stiffness of the truss is computed and decomposed. The load factor increment for the cycle as well as the displacements and reactions in the trial state at the end of the cycle are determined as in the geometrically nonlinear analysis (Galishnikova, 2009). The change in state of the bars is determined and recorded in flags whose value true has the following meaning:

e_{start}	the bar is elastic at the start of the load step
e_{end}	the bar is elastic at the end of the load step
d_c	at least one bar of the truss has changed state in the load step
d_e	at least one bar of the truss has turned elastic in the load step
d_p	at least one bar of the truss has deformed plastically in the load period

The flags are set with the logic shown in figure 3.

A bar which is elastic in a load step remains elastic at the end of the load step if the absolute value of its stress is less than the yield stress. Otherwise the bar yields at the end of the load step. The load reduction factor r for the bar is given by:

$$\begin{aligned} \sigma^{(t)} \geq 0: \quad r &= \frac{\sigma_y - \sigma^{(s)}}{\sigma^{(t)} - \sigma^{(s)}} \\ \sigma^{(t)} < 0: \quad r &= \frac{-\sigma_y - \sigma^{(s)}}{\sigma^{(t)} - \sigma^{(s)}} \end{aligned} \quad (6)$$

Consider a bar which is plastic during the load step. Small error bounds δ_e and δ_p are defined for the elastic and the plastic strain. Typical values are $\delta_e = 10^{-10}$ and $\delta_p = 10^{-6}$. If the stress at the start of the step is positive and the plastic strain increment $V\varepsilon_p$ is larger than δ_e or if the stress is not positive and $V\varepsilon_p$ less than δ_e the bar is plastic at the end of the load step. The bar has deformed plastically if $|V\varepsilon_p|$ exceeds δ_p . Otherwise the bar, contrary to the assumption at the start of the load step, was elastic in the load step and the flags are set accordingly.

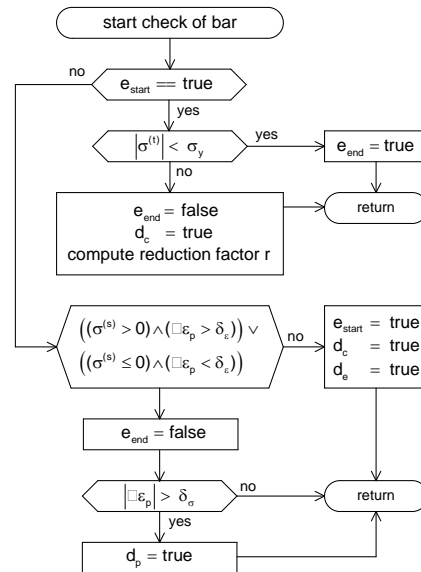


Fig. 3. Check of the state of a bar at the end of a cycle of iteration

If the state check at the end of the first cycle of iteration shows that none of the bars has changed state, the cycle is complete. If at least one bar has turned elastic the load step is repeated using the new bar states. Otherwise at least one bar has turned plastic and the smallest reduction factor r_{\min} is determined. After the trial state has been scaled with this factor the cycle is complete.

At the beginning of the second and all subsequent cycles of iteration in a load step the bar state is set equal to the state at the end of the previous cycle. The secant stiffness matrix is computed for the current displacement increments and the state of the bars. The procedure is continued as in the previous cycle. The iteration in the load step ends when the error norm of the trial solution is less than a specified limit value. The traversal of the load steps ends when the limit load is reached, or after a specified number of load steps have been performed. The limit load is reached when the maximum number of chord length reductions in the constant arc method does not lead to a positive definite secant matrix or to a sufficiently small error norm in the trial state of the truss in the load step.

Limit Analysis of a Pinned Arch

This example illustrates the application of the limit analysis described to the pinned circular arch in figure 4. The arch has a span of 28.0 m, a section height of 0.80 m and a width of 2.0 m. Analyses are performed for radii of the center line of the arch ranging from 20.0 to 200.0 m corresponding to elevations of 5.717 to 0.491 m of the crown above the supports. The number of bays is kept constant at 14, and all bays subtend the same angle at the center of the circle.

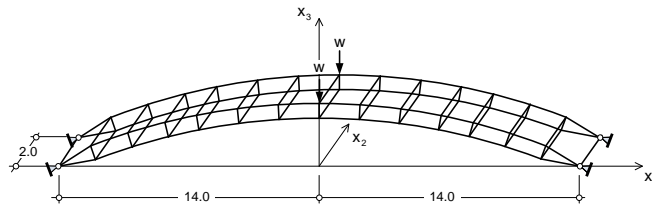


Fig. 4. Perspective of the arch truss (diagonals not shown)

Figure 4 shows only the chords and the ties of the arch. In the bays next to the supports there are crossed diagonals in the upper and the lower faces of the arch. In the other bays there are crossed diagonals in all four faces and in the cross-section normal to the center line of the arch.

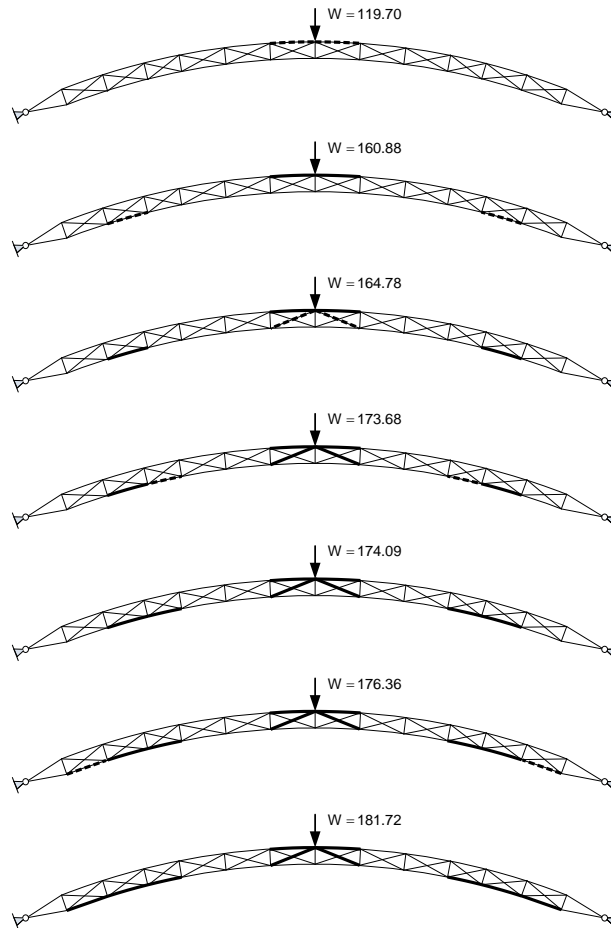


Fig. 5. Sequence of yielding of the bars of an arch truss with radius 30.0 m

All bars have an area of 0.008 m^2 except the two chords at each support which have an area of 0.012 m^2 . All bars have yield strength $2.4 \cdot 10^5 \text{ kN/m}^2$ and modulus of elasticity $2.1 \cdot 10^8 \text{ kN/m}^2$. The displacements at the four supports are null. The load

pattern consists of two loads $W=100$ kN applied in the downward direction at the crown of the arch in the upper face of the truss.

The arches have been analyzed with the Java implementation. Because the results of the limit analysis are symmetric with respect to plane $x_2=1.0$ only the results for elevation $x_2=0$ are shown in figure 5. Bars which are plastic during the load step leading to the specified load are shown continuous bold. Bars which yield at the specified load are shown dotted bold.

II. Results and Discussions

Figure 5 shows the sequence in which bars of a truss arch with radius 30.0 m yield as the load at the crown increases. The left part of the figure shows elevations of face $x_2=0$. The right part of the figure shows a plan of the two bays in the upper face of the arch next to the loaded nodes.

The cords in the upper face of the arch yield in the bays at the loaded nodes when the load reaches 65.9% of the ultimate load. At 88.5 % of the ultimate load the chords in the lower face yield in the third bay from the supports. The diagonals in the elevations of the arch which are incident at the loaded nodes yield at 90.7% of the ultimate load. At 95.6% of the ultimate load the plastic zone in the lower chords near the supports extends over an additional bay. Next the transverse tie in the upper face at the loads yields due to the forces in the crossed diagonals in the transverse section and the upper face. After the plastic zone in the lower face has extended over an additional bay at the supports, the ultimate load is reached when the diagonals in the upper face at the loaded nodes yield.

The ultimate load of the arch truss with a radius of 30.0 m is 181.72 kN. The arch fails because all bars which support the two loaded nodes in the x_1 direction have become plastic. The two loaded nodes can therefore displace in the x_1 direction without an increase in load. This state is detected in the algorithm because the regularity of the stiffness matrix of the truss is monitored. The matrix becomes singular in the configuration which carries the ultimate load.

The vertical downward displacement of the crown nodes in the upper face of the arch is shown in figure 6 as a function of the load. The maximum displacement is 89.5 mm for a load of 181.7 kN. It is noted that the tangent to the displacement-load curve is not horizontal at the ultimate load. This is due to the failure mode of the arch: the nodes under the load become locally unstable, but there is no mechanism or loss of stability of the structure as a whole.

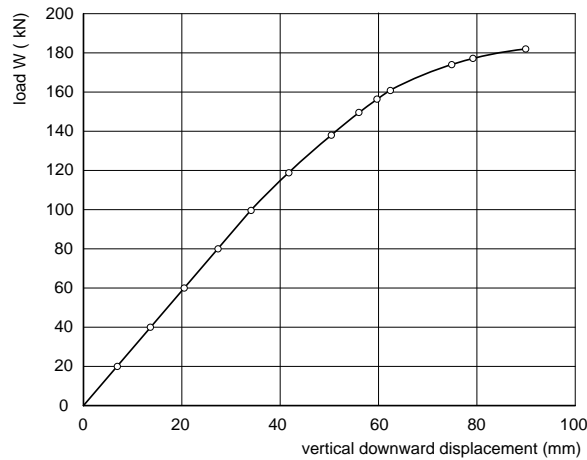


Fig. 6. Vertical downward displacement of the loaded nodes in Fig. 5

The vertical downward displacement of the crown nodes in the upper face of the arch is shown in figure 6 as a function of the load. The maximum displacement is 89.5 mm for a load of 181.7 kN. It is noted that the tangent to the displacement-load curve is not horizontal at the ultimate load. This is due to the failure mode of the arch: the nodes under the load become locally unstable, but there is no mechanism or loss of stability of the structure as a whole.

The plastic strain in the bars of the truss is shown in figure 7. The largest plastic strain of -2228×10^{-6} m/m occurs in the upper chords like bar b_{104} at the loaded nodes. The next highest plastic strain of -1249×10^{-6} m/m occurs in the diagonals of the vertical faces like bar b_{109} which support the loaded nodes. Tensile plastic strains of 791×10^{-6} m/m occur in the transverse diagonal b_{119} which connects the two loaded nodes. Bars b_{33} and b_{51} are the lower chords in the third and fourth bay from the left support. Their plastic strains are considerably less than the strains in the upper chords at the loads.

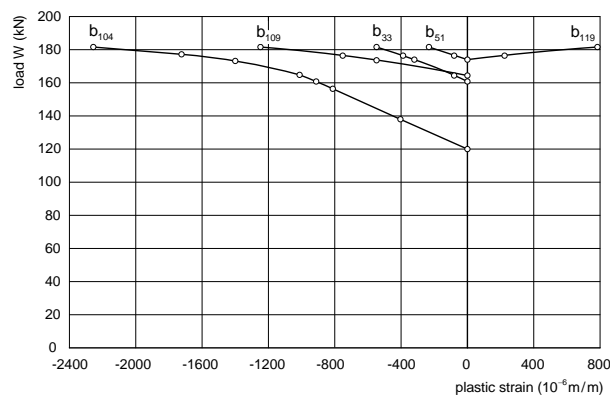


Fig. 7. Plastic strain in the bars of the arch truss

The variation of the maximum load factor λ_{\max} with the height of the center line of the arch at the crown above the supports is shown in Figure 8. For shallow arches the factor increases rapidly with the height. When the height reaches 7% of the span of 28.0 m the rate of increase of λ_{\max} becomes significantly less. For heights in excess of 20% of the span the increase of λ_{\max} becomes small.

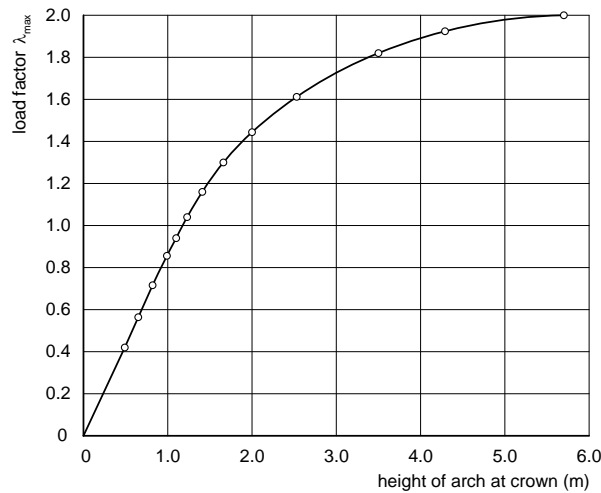


Fig. 8. Variation of the maximum load factor with the height of the arch

The maximum horizontal reaction at the supports does not increase continuously with the height of the arch, but rather reaches a maximum for a radius of 70.0 m when the height of the arch is 5.1% of its span. The ratio of the horizontal reaction to the load acting on the arch increases continuously with the radius.

The arch trusses which have been investigated do not buckle elastically. If the yield strength of the material is set to an artificial high value so that plasticity is prevented, the shallow arches buckle for the following load factors λ_{elastic} :

r= 90.0m	$\lambda_{\text{elastic}} = 2.603$	$\lambda_{\max} = 0.942$
r= 100.0m	$\lambda_{\text{elastic}} = 2.064$	$\lambda_{\max} = 0.856$
r= 120.0m	$\lambda_{\text{elastic}} = 1.442$	$\lambda_{\max} = 0.716$
r= 150.0m	$\lambda_{\text{elastic}} = 0.970$	$\lambda_{\max} = 0.566$

The results show that plasticity reduces the load carrying capacity of a truss arch significantly even if the arch is shallow.

III. Conclusions

The example of the arch truss demonstrates that direct limit analysis of space trusses with large displacements can be implemented successfully on the Java platform.

The method of analysis determines the exact load for each change of state in any bar of the truss. This detail of information permits a precise analysis of the behavior of the truss and the events that lead up to the collapse of the truss at the ultimate load.

For example, it was determined that failure of the arch truss is not due to an overall instability, but rather to a local instability of the loaded nodes. This knowledge can be used to improve the design of the structure. The computer application is suitable as a test platform for a broad spectrum of investigations into elastic-plastic truss behavior. The time required for the limit analysis of the arch on a conventional laptop computer is 0.010 seconds. The structure has 56 nodes and 238 bars. It was analyzed for 15 configurations. The band width of the system equations is approximately 10% of the dimension of the equations.

The computational effort for a limit analysis is approximately proportional to the time required for the solution of the system equations and to the number of changes in state of the bars that occur before the limit configuration is reached. An extrapolation of the measured computational effort indicates that the time required for a limit analysis a truss with 500 nodes, 2000 bars and 100 configurations is of the order or one minute. Before this capacity to analyze larger structures can be utilized, an interactive graphic user surface must, however, be implemented to support the interpretation of the computed results which are very voluminous.

IV. Acknowledgement

This research work was supported by the Ministry of Education and Science of the Russian Federation (Agreement No. 02.A03.21.0008).

References

- I. Bathe, K.J., Polourchi, S. (1979). Large Displacement Analysis of Three-Dimensional Beam Structures. *International Journal for Numerical Methods in Engineering*, 14: 961-986.
- II. Bathe, K.J., (1982) "Finite Element Procedure in Engineering Analysis", Prentice-Hall, 1982.
- III. Belytscko, T., Liu, W., Moran, B. (2000). *Nonlinear Finite Elements for Continua and Structures*. J Wiley & Sons. ISBN 0-948-749-261.
- IV. Drucker, D.C. (1958). Plastic Design Methods – Advantages and Limitations. *Transactions, Soc. nav. Arch. mar. Engrs* 65, P. 172.
- V. Galishnikova, V.V. (2009). Derivation of the governing equations for the problem of geometrically nonlinear deformation of space trusses on the basis of unified approach. *J. of Volgograd State University for Architecture and Civil Engineering. Civil Eng. & Architecture*, 14(33): 39-49 (in Russian).
- VI. Galishnikova, V.V. (2009). Finite element formulation of the problem of geometrically nonlinear deformations of space trusses. *Journal of Volgograd State University for Architecture and Civil Engineering. Civil Eng. & Architecture*, 14(33), 50-58 (in Russian).

- VII. Galishnikova, V.V. (2009). Modification of the constant arc length method based on the secant matrix formulation. *Journal of Moscow State University of Civil Engineering*, 2: 63-69 (in Russian).
- VIII. Galishnikova, V.V. (2007). Finite element modeling of geometrically nonlinear behavior of space trusses. *Journal of Civil Engineers. Saint-Petersburg University of Architecture and Civil Engineering*, 2(11): 101-106 (in Russian).
- IX. Galishnikova, V.V. (2007). Algorithm for geometrically nonlinear stability analysis of space trussed systems. *Proceedings of the XXVII Russian School "Science and Technology"*. Moscow: Russian Academy of Science, 235-244 (in Russian).
- X. Galishnikova V.V. (2015). Generalized geometrically nonlinear theory and numerical deformation and stability analysis of space trusses. Dissertation submitted for the degree of Dr. of Tech. Science. Moscow State University of Civil Engineering, 2015.
- XI. Heidari, A, Galishnikova, V.V. (2014). A Review of Limit Load and Shakedown Theorems for the Elastic-Plastic Analysis of Steel Structures. *Structural Mechanics of Engineering Constructions and Buildings*, 3: 3-18.
- XII. Vu Duc Khoi. (2001). Dual limit and shakedown analysis of structures. Doctoral Thesis, University of Liege.